



1 Foliar nutrient uptake from dust sustains plant nutrition

2 Anton Lokshin^{1,2*}, Daniel Palchan², Elnatan Golan³, Ran Erel³, Daniele Andronico⁴, and Avner Gross¹

3 1. The Department of Environment, Geoinformatics and Urban planning Sciences, Ben Gurion University of the
4 Negev; Beer Sheva, Israel.

5 2. The Department of Civil Engineering, Ariel University; Ariel, Israel.

6 3. Institute of Soil, Water and Environmental Sciences, Gilat Research Center, Agricultural Research Organization;
7 Gilat, Israel.

8 4. Istituto Nazionale di Geofisica e Vulcanologia, Sezione di Catania-Osservatorio Etneo, Rome, Italy.

9

10 * **Corresponding author:** Lokshinantanton@gmail.com

11

12

13

14

15

16

17

18

19

20

21

22

23

24

25

26

27

28

29

30

31

32



33 Abstract

34 Mineral nutrient uptake from soil through the roots is considered the exclusive nutrition pathway for vascular
35 terrestrial plants. Recently, desert dust was discovered as an alternative nutrient source to plants, through direct
36 uptake from dust deposited on their foliage. Here we studied the uptake of nutrients from freshly deposited desert
37 and volcanic dusts by chickpea plants under ambient and future elevated levels of atmospheric CO₂, through the
38 roots and directly through the foliage. We found that within weeks, chickpea plants acquired phosphorus (P) from
39 dust only through foliar uptake under ambient conditions, and P, Iron (Fe) and Nickel (Ni) under elevated CO₂
40 conditions, significantly increasing their growth. Using additional chickpea variety with contrasting leaf properties
41 we have shown that the foliar nutrient uptake pathway from dust is facilitated by leaf surface chemical and
42 physiological traits such as low pH and trichome densities. We analyzed Nd radiogenic isotopes extracted from
43 plant tissues after dust application to assess the contribution of mineral nutrients that were acquired through the
44 foliage. Our results suggest that foliar mineral nutrient uptake from dust is an important pathway, that may play
45 an even bigger role in an elevated CO₂ world.

46

47

48

49

50

51

52

53

54

55

56

57

58

59

60

61

62

63

64 **Keywords:** plant nutrition; Nd isotopes; hidden hunger; foliage; elevated CO₂

65



66 Introduction

67 Vascular plants obtain carbon (C) from the atmosphere and most of their mineral nutrients from the soil. Hence,
68 it is generally thought that mineral nutrients such as phosphorus (P), potassium (K), iron (Fe), and other macro
69 and micronutrients are acquired predominantly through the plant's roots system (Marschner et al., 1997). Evidence
70 gathered in recent decades demonstrates that the atmosphere is an important source for mineral-nutrients to
71 terrestrial ecosystems via dust deposition (Chadwick et al., 1999; Goll et al., 2023; Gross et al., 2015; Van
72 Langenhove et al., 2020; Okin et al., 2004; Palchan et al., 2018). The concentration of P (and other nutrients) in
73 mineral atmospheric particles such dust and volcanic ash are enriched relative to most soils and are important
74 plant nutrient source, especially when soil fertility is low or in dusty regions (Arvin et al., 2017; Bauters et al.,
75 2021; Ciriminna et al., 2022; Eger et al., 2013; Gross et al., 2016b). In a montane environment in California, dust
76 P contribution to plants was documented to outpace the contribution from weathering of host bedrock (Arvin et
77 al., 2017). In a recent study we discovered that certain crop plants can gain P directly from the atmospheric dust,
78 via particles that accumulate on their leaves (Gross et al., 2021a; Lokshin et al., 2024b). Over short time scales,
79 foliar uptake was found as the only P uptake pathway from biomass fire ash particles (while the roots played a
80 negligible role (Lokshin et al., 2024a, b). These recent findings highlights the need to better understand the role
81 of the contribution of nutrient uptake from dust through the foliage (i.e., direct foliar nutrient uptake), a process
82 that has been traditionally overlooked and has never been quantified before, even though foliar fertilization has
83 been a well-known agricultural practice for many decades (Fageria et al., 2009; Ishfaq et al., 2022; Bukovac &
84 Wittwer, 1957; Wittwer & Teubner, 1959). In the context of climate change, the foliar pathway may be even more
85 pronounced for plants that will grow under elevated CO₂ (eCO₂) conditions because of two documented
86 phenomena: the 'dilution' effect, where accumulation of C exceeds that of mineral nutrients (Loladze, 2014), and
87 partial inhibition of key root uptake mechanisms (Gojon et al., 2023), together with soil fertility degradation (Lal,
88 2009; St.Clair and Lynch, 2010). These changes will drive plants to adapt and search for other nutrient uptake
89 pathways. The use of the foliar pathway under eCO₂ may offset the alarming phenomenon where an increasing
90 production of carbohydrates causes dilutes the concentration of macro and micronutrients such as P, Fe, calcium
91 (Ca), magnesium (Mg), K, zinc (Zn), copper (Cu), nickel (Ni) and others that are vital for the floral ecological
92 systems (Clarkson and Hanson, 1980) and for their dependent human and livestock nutrition (Lal, 2009; Loladze,
93 2002; Lowe, 2021). In this experiment, we cultivated C3 chickpea plants (specifically the 'Zehavit' variety, a
94 widely grown modern cultivar) under both current atmospheric CO₂ concentrations and elevated CO₂ conditions
95 in a controlled glasshouse environment. The primary objective was to demonstrate, describe and quantify nutrient
96 uptake via the leaves. We introduced two distinct types of mineral dust to the plants, applying them either to the
97 surface near the root zone or directly onto the leaves. The two dust types were representative of major atmospheric
98 particulate matter sources, namely desert-derived dust and volcanic ash (referred to as "dust" hereafter), with
99 average annual global emissions estimated at 3,000 Tgy⁻¹ and 300 Tgy⁻¹, respectively (Kok et al., 2021;
100 Langmann, 2013a).

101 We studied leaf traits that facilitate the foliar nutrient uptake from dust, its impact on plants' ionome (i.e., plant
102 elemental status), and used Nd radiogenic isotopes, present within the dust particles and characterized by distinct
103 isotopic values, to quantify the contribution of the foliar pathway. In addition, we used a non-responsive genotype,
104 'CR934', of the wild progenitor *C. reticulatum*, to study the impact of dust deposition on plant nutrition and



105 compare leaf properties under dust foliar fertilization between the modern chickpea cultivar and its wild
106 counterpart.

107

108

109

110 **Materials and Methods**

111 **Experimental design**

112 To study the impact of dust deposition on plant nutrition, two chickpea genotypes (*Cicer*) from the Hebrew
113 University of Jerusalem chickpea collection were selected based on preliminary experiments, showing contrasting
114 response to foliar dust application (Gross et al., 2021b). The non-responsive genotype: ‘CR934’, of the wild
115 progenitor *C. reticulatum* accession, sampled near Savur, Turkey. And the responsive genotype ‘Zehavit’ that is
116 a modern, high yield line, and considered popular among the Israeli growers. To test the biogeochemical response
117 of the foliar nutrient uptake we used the ‘Zehavit’ genotype. Experiments were conducted at Gilat Research Center
118 in southern Israel (31°21’ N, 34°42’ E) in two separate glasshouse rooms. In one room we set the CO₂
119 concentration to the ambient 412 ppm (aCO₂) and in the other room to elevated 850 ppm (eCO₂), simulating
120 current and future earth CO₂ concentrations based on high emissions scenario (business as usual, SSP 8.5, IPCC,
121 2021). Following germination, plants were cultivated in 72 pots containing inert media (perlite 206, particle size
122 of 0.075–1.5 mm; Agrekal, HaBonim, Israel). The pot size was 3 litter, with sufficient room for root growth during
123 the experimental period. The description of the growing conditions and fertigation nutrient supplement is provided
124 in Lokshin et al. (2024a).

125 At 14 days after germination, when plants were early in the vegetative phase (two or three developed leaves), we
126 changed the nutrient solution of 60 out of the 72 pots to P deficient fertigation (P concentration of 0.1 mg L⁻¹) to
127 create P starvation (-P treatment). Preliminary tests showed that our -P deficient media allows chickpea plants to
128 continue their growth cycle and increase their responsiveness for dust application and eCO₂ condition (Gross et
129 al., 2021, Lokshin et al., 2024). The remaining 12 pots continued to receive the full P sufficient nutrient media
130 (+P treatment). Plants fertigated with -P solution started to show P-deficiency symptoms such as chlorosis of
131 mature leaves, slight symptoms of necrotic leaf tips and an overall decrease in biomass accumulation at 35 days
132 after germination. At this stage we applied desert dust and volcanic ash on the -P plants.

133 Of a total number of plants (72) 48 were treated with dust and 24 served as untreated control group. Twenty-four
134 plants were applied with dust on their foliage by manually sprinkling dust through a 63µm sieve in proximity to
135 the foliage and 24 plants received root treatment by applying dust through a 63 µm sieve on the surface of the pot,
136 followed by gentle mixing of the surface to sink the dust particles deeper to enhance the physical contact between
137 the roots and the particles, thereby increasing the chances of having a more significant impact. Among the control
138 plants, 12 plants received the +P fertigation and 12 additional plants received -P fertigation. Each treatment group
139 was divided into two CO₂ levels, 36 plants in each CO₂ growing room. The plants were harvested 10 days after
140 the last dust application (55 days after germination). To ensure that nutrients from dust particles were not washed
141 by the irrigation during the experiment, we monitored the total P (i.e., P that dissolves in strong acid) in the water
142 that drained from the pots (Longo et al., 2014; Gross et al., 2015) throughout the experiment.



143 We performed a parallel experiment under aCO₂ where we grew six additional plants, in larger 5 L pots, filled
144 with soil, to test whether our findings also apply to natural soil conditions (Fig. S1).

145 **Mineral dust material**

146 We applied plant foliage and the area near plants' roots, with desert dust and volcanic ash, the two main mineral
147 dust types in the atmosphere (Langmann, 2013b). To achieve enough mass for our experiment, we produced dust
148 analogs from surface desert soil and surface volcanic ash soil, following common procedures described by others
149 (Gross et al., 2021b; Stockdale et al., 2016). The desert dust analog surface soil was collected from the southern
150 Israel Negev desert (30°32'N 34°55'E) (Gross et al., 2021b). Chemical and mineralogical properties of the
151 resulted dust are comparable to dust collected in the Sahara and other places in the Middle East (Gross et al.,
152 2016a; Palchan et al., 2018). The volcanic ash analog was collected from Mount Etna (Sicily, Italy) two month
153 after the eruption of 21 February 2022. The ash was taken from the upper cable car station "Funivia dell'Etna"
154 (37°70'N, 14°99'E). The samples were then processed through a setup of sieves to achieve a particle size smaller
155 than 63 μm that are considered windblown (Guieu et al., 2010). The chemical and mineralogical properties of the
156 dust analogs are presented in Table 1.

157 To mimic dust deposition which typically occurs during a few major desert storms or volcanic eruption each year,
158 we applied the dust in two equivalent doses between 35-42 days after germination. Total application mass was 3
159 g per plant, to simulate the total dust deposition per m² for an average growth period in southern Israel (Gross et
160 al., 2021b). Dust treatments were done either directly on the foliage while covering the pot, preventing the dust
161 from touching the roots, or directly on the roots where the pots were subsequently covered with nylon to equalize
162 conditions with the foliage treated plants. Afterwards, the plants were left undisturbed with the settled dust
163 particles on their foliage or surface of the root area.

164

165 **Plant biomass and elemental analysis**

166 After harvesting, the plants were separated for roots and shoots, washed in 0.1M HCl and rinsed three times in
167 distilled water to remove dust particle residue (Gross et al., 2021; Lokshin et al., 2024a). To ensure that the
168 washing procedure removed all the applied dust particles from the leaf surfaces, we scanned surfaces of randomly
169 selected dusted and washed leaves with SEM-EDS which combines scanning electron microscope and energy-
170 dispersive X-ray spectroscopy to detect and analyze materials. After washing, plant tissue was dried, weighed and
171 root and shoot biomass were recorded. Afterwards, the dry shoot material was ground to powder and dry ashed at
172 550 °C in a furnace for four hours (Tiwari et al., 2022). Approximately 1g of the ashed material was subsequently
173 dissolved using 1 mL concentrated HNO₃ to achieve a clear solution. To prepare the dust types for elemental
174 analysis, the samples were dissolved on a hotplate by sequential dissolution using concentrated HNO₃, HF, and
175 HCl, resulting in clear solutions (Palchan et al., 2018). The elemental composition of the plants, dusts and nutrient
176 solution were analyzed at the Hebrew University using ICP-MS (Agilent 8900cx; Agilent Technology). Prior to
177 analysis, the ICP-MS was calibrated with a series of multi-element standard solutions (1 pg/mL - 100 ng/mL
178 Merck ME VI) and standards of major metals (300 ng/mL - 3 mg/mL). Internal standard (50 ng/mL Sc and 5 ng/mL
179 Re and Rh) was added to every standard and sample for drift correction. Standard reference solutions (USGS SRS



180 T-207, T-209) were examined at the beginning and end of the calibration to determine accuracy. The calculated
181 accuracies for the major and trace elements are 3% and 2%, respectively.

182 **Leaf surface pH**

183 Leaf surface pH was measured by manually attaching a portable pH electrode designed for flat surfaces (HI-1413;
184 HANNA pH instruments) onto the surface of three leaves from each plant. The measurements were performed
185 four times throughout the growing season (19, 24, 35 and 40 DAG) in the morning, two hours after sunrise.
186

187 **Trichome density**

188 Trichome density was determined in four young, fully developed leaves from four different plants per variety in
189 the P- treatment only (n=16). Leaves were scanned in a scanning electron microscope (VEGA3; Tescan, Czech
190 Republic). From each leaf, three photos of a 1mm² field were taken, and glandular and regular trichomes were
191 counted.
192

193 **Leaf exudates**

194 For analysis of the organic exudates, 2g of fresh leaves were sampled randomly from the P+ and P- treatments
195 before harvesting. The leaves were rinsed in 2 ml of distilled water and methanol (50:50) for 10 s. The extracted
196 surface metabolites were supplied with 50 µL of internal standard (ribitol, 0.2 mg ml⁻¹) and stored at -80°C until
197 analysis. Before analysis, the extracted samples were vacuum dried overnight at 35°C. The dried material was
198 redissolved in 40 µl of 20 mg mL⁻¹ methoxamine hydrochloride (CH₃ONH₂ HCl) in pyridine (C₅H₅N) and
199 derivatized for 90 min at 37°C, followed by a spike of 70 µL MSTFA (*N*-methyl-*N*-(trimethylsilyl)
200 trifluoroacetamide (CF₃CON(CH₃)Si(CH₃)₃) at 37°C for 30 min. The dissolved metabolites were then introduced
201 to a mass spectrometry gas chromatograph (Agilent 6850 GC/5795C; Agilent Technology) for analysis. The
202 metabolites were detected by a mass spectrometer, where 1 µL of each sample was injected in split-less mode at
203 230°C to a helium carrier gas at a flow rate of 0.6 mL min⁻¹. GC processing was carried out using an HP-5MS
204 capillary column (30 m 9 0.250 mm 9 0.25 µm) and the spectrum was scanned for *m/z* 50–550 at 2.4 Hz. The ion
205 chromatograms and mass spectra obtained were evaluated using the MSD CHEMSTATION (E.02.00.493)
206 software, and sugars and amino acids were identified via comparison of retention times and mass spectra with
207 certified GC plant metabolite standards (Sigma Aldrich).
208

209 **Nd isotope chromatography and analysis**

210 Nd isotopes were measured on the dusts and in the above ground plant material at the end of the experiment. Nd
211 was extracted from the samples using TRU followed by LN-spec resins (Palchan et al., 2013). Measurements of
212 the isotopic ratios were performed using a Thermo Neptune multi-collector ICP-mass spectrometer at the
213 Weizmann Institute of Science. A JNdi Nd standard bracketed the samples, resulting with ¹⁴³Nd/¹⁴⁴Nd value of
214 0.512035 ± 1⁻⁵ (2σ, n=60). The data was normalized to ¹⁴³Nd/¹⁴⁴Nd = 0.512115 (Tanaka et al., 2000). Rock
215 standards samples of BCR-2 were dissolved and measured along with the plant and dust samples yielding



216 $^{143}\text{Nd}/^{144}\text{Nd}$ value of $0.512628 \pm 6 (2\sigma)$ that agrees with $^{143}\text{Nd}/^{144}\text{Nd} = 0.512637 \pm 13$ value of BCR-2 (n=3)(Jweda
217 et al., 2016). The Nd isotopic ratio is expressed as:

218

219
$$\varepsilon Nd = \left(\frac{\left(\frac{^{143}\text{Nd}}{^{144}\text{Nd}} \right)_{\text{Sample}}}{\left(\frac{^{143}\text{Nd}}{^{144}\text{Nd}} \right)_{\text{CHUR}}} - 1 \right) * 10,000$$

220

221 where the present value of $^{143}\text{Nd}/^{144}\text{Nd} = 0.512638$ in CHUR (Wasserburg et al., 1981). A sample isotopic
222 characterization is given in SI Table 4. The percent contribution of Nd within the leaves that comes either from
223 desert dust or volcanic ash (foliar contribution) was calculated using simple mixing equation of two components:

224

225
$$\% \text{ Foliar contribution} = \frac{\varepsilon Nd_{\text{sample}} - \varepsilon Nd_{\text{control}}}{\varepsilon Nd_{\text{end member}} - \varepsilon Nd_{\text{control}}} * 100$$

226

227 Where $\varepsilon Nd_{\text{sample}}$ refers to plants that were treated either with desert dust or volcanic ash with, $\varepsilon Nd_{\text{control}}$ refers to
228 the untreated control plants and $\varepsilon Nd_{\text{end member}}$ are the measured end member values of -10.3 for desert dust or 4.5
229 value for volcanic ash (Table SI-4 & Fig. 4).

230

231 **Mineralogical analysis**

232 Mineralogical composition of the dusts was determined with an X ray powder diffraction (XRD) using a
233 Panalytical Empyrean Powder Diffractometer equipped with a position sensitive X'Celerator detector. Cu K α
234 radiation (k = 1.54178_A) at 40 kV and 30 mA. Scans were done over a 2h period, between 5° and 65° with an
235 approximate step size of 0.033°.

236

237 **Statistical Analysis**

238 Treatment comparisons for all measured parameters were tested using post-hoc Tukey honest significant
239 difference (HSD) tests (P < 0.05). The significant differences are denoted using different letters in the figures.
240 The standard errors of the mean in the vertical bars (in the figures) were calculated using GraphPad Prism version
241 9.0.0.

242

243 **Results**

244 **Plant biomass and total P under aCO₂ and eCO₂**

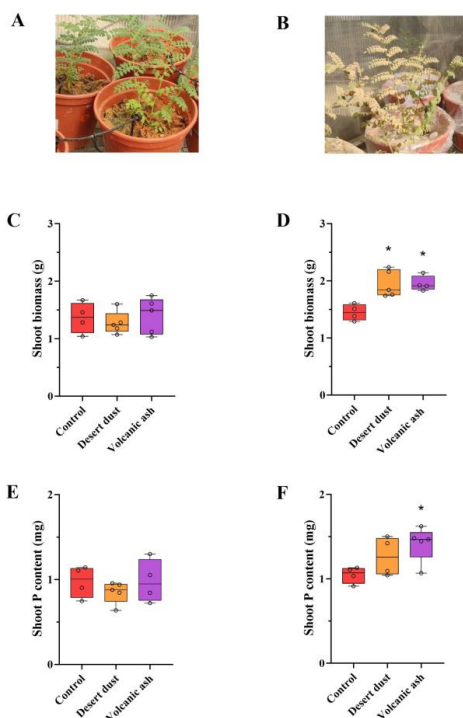
245 P starvation did not reduce P concentration in shoots but rather decreased shoot biomass gain. In addition, eCO₂
246 had no impact on P concentration or shoot biomass gain in the control -P plants, but significantly increased shoot



247 biomass gains in +P treated plants (Table 1). Thus, the treatment effects are reflected by changes in total plant P
248 (concentration multiplied by shoot biomass). The impact of desert and volcanic dust application on plants' foliage
249 was reflected by the increase of their total P content through shoot biomass gain rather than through changes in
250 shoot P concentration. Under aCO₂ conditions, desert dust application resulted in shoot biomass and total P content
251 increases of 35% and 21%, respectively, and volcanic ash application resulted in 28% and 35% increases,
252 respectively (Fig. 1 d,f). The root-treated plants did not show any increases in the shoot biomass or total P content
253 (Fig. 1 c,e). These trends are also seen in the eCO₂ conditions of 850 ppm atmospheric CO₂ experiment. Desert
254 dust application resulted in shoot biomass and total P content increases of 29% and 20%, respectively, and
255 volcanic ash application resulted in 62% and 51% shoot biomass increases, respectively (Fig. 2 d, f). Similarly,
256 the root-treated plants did not show any increases in the shoot biomass or total P content (Fig. 2 c, e). Unlike the
257 shoots, no significant changes of the biomass of the roots were detected across all treatments, thus changes in the
258 root shoot ratio reflect variations in shoot biomass rather than root biomass (Table 1).

259

Root treatment 412 ppm Foliar treatment 412 ppm



260

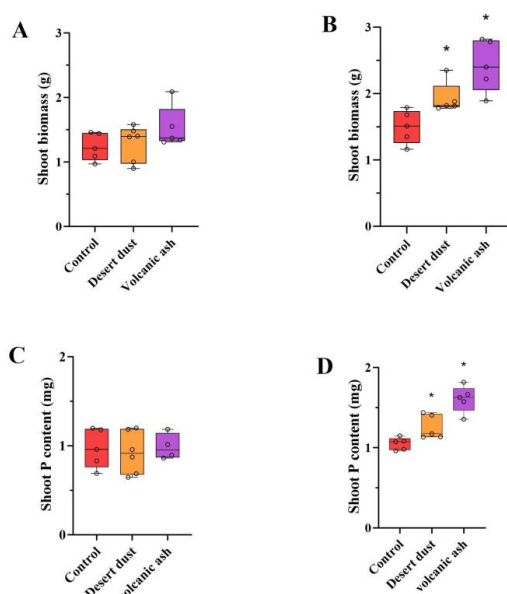
261 **Fig. 1** Biomass and total P content increases due to dust application treatments at aCO₂ of 412ppm. (a) Image of experiment
262 setting of the root treatment. (b) Image of experiment setting of foliar treatment. (c) Shoot biomass of root treated plants. (d)
263 Shoot biomass of foliar treated plants. (e) Shoot total P content of root treated plants. (f) Shoot total P content of foliar treated
264 plants. The asterisk denotes statistically significant difference from the control. The biomass and total P content in the root



265 treated plants do not show increases compared with the control groups. However, the foliar treatment of both desert dust and
266 volcanic ash caused significant increases in the shoot biomass and total P content. This implies that plants acquire P from fresh
267 dust deposits on their foliage and not from the root system. Red color represents control plants, orange desert dust treatment
268 and purple volcanic ash treatment.

269

Root treatment 850 ppm Foliar treatment 850 ppm



270

271 **Fig. 2** Biomass and total P content increases due to dust application treatments at eCO₂ of 850ppm. (a) Shoot biomass of root
272 treated plants. (b) shoot biomass of foliar treated plants. (c) Shoot total P content of root treated plants. (d) Shoot P content of
273 foliar treated plants. The asterisk denotes statistically significant difference from the control. The biomass and total P content
274 in the root treated plants do not show increases compared with the control groups. However, the foliar treatment of both desert
275 dust and volcanic ash caused significant increases in the shoot biomass and total P content. This implies that plants acquire P
276 from fresh dust deposits on their foliage and not from the root system. Red color represents control plants, orange desert dust
277 treatment and purple volcanic ash treatment.

278 Elemental analysis of the plants

279 The concentrations of selected micro and macro nutrients that build plants ionome, together with plants shoot
280 biomass, are given in Table 1.



281 **Table 1** Total elemental analysis of the plants (*Cicer arietinum* cv 'Zehavit') fertilizers and dusts (ICP-MS analysis). The
 282 concentration of the different micro and macro elements are shown in ppm and plant biomass in g.

Plant material (ppm)	Shoot biomass (g)	Root biomass (g)	Root/Shoot ratio	Mg	P	K	Ca	Mn	Fe	Ni	Cu	Zn
Control -P 412 #1	1.03	0.91	0.89	2749	715	21928	7257	52	75	1.3	2.9	22.9
Control -P 412 #2	1.29	0.95	0.74	2828	860	21147	7266	45	112	2.3	10.8	23.5
Discarded plant												
Control -P 412 #4	1.51	1.36	0.90	2814	686	23832	7462	33	97	2.4	3.7	21.9
Control -P 412 #5	1.38	1.22	0.88	2863	663	21883	7684	38	94	1.0	2.7	23.7
Control -P 412 #6	1.61	1.39	0.87	2513	704	19705	6531	19	69	1.3	3.3	23.4
Control -P 850 #1	1.35	1.02	0.75	2585	727	23099	6323	22	71	1.0	1.9	23.4
Control -P 850 #2	1.16	1.02	0.88	3848	827	27768	7922	61	79	0.2	2.8	38.9
Control -p 850 #3	1.79	1.39	0.78	2785	607	20121	7118	50	67	1.2	2.5	24.9
Discarded because plant did not grow/withered												
Control -P 850 #5	1.51	1.25	0.82	2847	759	27272	7572	21	88	2.2	4.7	26.4
Control -P 850 #6	1.68	1.44	0.86	3180	640	24460	8732	31	93	1.6	2.9	29.1
desert dust foliar-treated 412 ppm #1	2.24	1.65	0.74	2490	1458	23743	7040	47	125	0.9	2.6	21.9
desert dust foliar-treated 412 ppm #2	1.74	1.44	0.83	2450	628	19416	6715	29	102	0.6	2.0	19.2
desert dust foliar-treated 412 ppm #3	1.76	1.57	0.90	2326	855	17424	6576	27	97	1.0	2.3	20.5
desert dust foliar-treated 412 ppm #4	2.16	1.87	0.87	2224	658	17576	6060	28	101	1.1	3.3	23.2
desert dust foliar-treated 412 ppm #5	1.84	1.33	0.72	2611	566	21928	6817	40	116	1.1	3.0	20.3
Discarded because plant did not grow/withered												
desert dust foliar-treated 850 ppm #1	1.82	1.18	0.65	2274	626	21092	6599	26	151	2.2	2.8	22.1
desert dust foliar-treated 850 ppm #2	1.78	1.58	0.89	2083	808	20320	5877	34	125	1.9	3.7	17.1
Discarded because plant did not grow/withered												
desert dust foliar-treated 850 ppm #4	2.35	1.52	0.65	2182	482	20380	7336	43	135	2.2	3.4	18.6
desert dust foliar-treated 850 ppm #5	1.81	1.57	0.87	2995	648	24419	8366	39	169	2.4	3.5	25.0
desert dust foliar-treated 850 ppm #6	1.88	1.92	1.02	2848	749	24303	8087	39	144	3.4	3.2	21.1
volcanic ash foliar-treated 412 ppm #1	1.91	1.44	0.75	2499	755	20825	6058	34	137	0.6	3.0	18.1
volcanic ash foliar-treated 412 ppm #2	2.14	1.74	0.81	2655	691	22032	6993	50	317	1.5	3.0	25.7
volcanic ash foliar-treated 412 ppm #3	1.41	1.00	0.71	2524	757	18830	8067	49	148	1.0	2.9	20.8
Discarded because plant did not grow/withered												
volcanic ash foliar-treated 412 ppm #5	1.83	1.30	0.71	2814	800	23818	7121	40	177	1.4	3.5	23.7
volcanic ash foliar-treated 412 ppm #6	1.92	1.49	0.78	2811	844	23122	7359	47	162	1.1	3.5	23.0
Discarded because plant did not grow/withered												
volcanic ash foliar-treated 850 ppm #2	2.22	1.85	0.83	2289	818	22549	6623	34	149	0.6	3.0	19.9
volcanic ash foliar-treated 850 ppm #3	2.82	2.48	0.88	2365	558	23525	6848	41	373	2.4	3.4	18.2
volcanic ash foliar-treated 850 ppm #4	2.40	2.19	0.91	2717	692	25778	7020	60	173	1.0	3.5	26.1
volcanic ash foliar-treated 850 ppm #5	1.89	1.38	0.73	2584	718	24440	6722	43	140	0.7	3.0	23.5
volcanic ash foliar-treated 850 ppm #6	2.78	2.37	0.85	2689	585	21384	7224	59	181	0.4	3.3	27.6
Control +P 412 #1	10.46	3.33	0.32	5138	2465	30660	9429	79	161.3	1.1	5.1	51.2
Control +P 412 #2	11.69	5.07	0.43	3729	2101	26096	7892	49	111.1	0.4	4.6	37.2
Control +P 412 #3	11.47	4.44	0.39	6540	2148	29291	9076	69	88.9	0.7	4.3	43.5
Control +P 412 #4	10.06	3.39	0.34	3322	1982	23933	6871	36	82.0	0.4	3.8	28.4
Control +P 412 #5	10.76	3.94	0.37	3415	1804	23800	6970	44	95.5	0.4	4.1	33.1
Control +P 412 #6	10.02	3.88	0.39	5147	2240	27966	8384	50	95.0	0.5	4.6	38.5
Discarded plant												
Control +P 850 #2	13.40	7.24	0.54	3759	2253	26837	7886	59	91.4	0.8	3.8	32.6
Discarded plant												
Control +P 850 #4	17.17	7.29	0.42	3202	2196	25021	8052	68	96.6	0.8	5.9	30.5
Control +P 850 #5	17.51	10.85	0.62	3633	2258	27403	8860	67	97.0	0.7	4.1	31.7
Control +P 850 #6	15.86	6.55	0.41	5488	2959	30362	11394	100	109.5	0.9	4.9	50.5
Fertilizers and dusts (ppm)												
+P fertilizer				1226	713	6000	11	76	151	0.4	5.6	50.1
-P fertilizer				1214	35	7808	7	70	136	0.4	5.1	47.5
Desert dust				6513	1387	8673	136081	245	12745	18.0	10.0	39.0
Volcanic ash #1				23534	1669	12514	64461	1097	63736	49.5	118.6	80.0
Volcanic ash #2				22648	1788	12056	61628	1066	61903	48.3	115.6	73.7

283
 284
 285
 286
 287
 288
 289
 290

Physiological adaptations toward foliar uptake

291 The domesticated variety 'Zehavit' showed a strong response to the foliar treatment with up 35% increased
 292 biomass compared to the control group, whereas the wild variety CR934 showed up to 5% increases compared
 293 with the control group (Fig. 3a). The leaf pH of the Zehavit was 1.15 and of the CR934 it was 2.7 (Fig. 3b),



294 trichome density, both glandular and non-glandular, were higher in the Zehavit compared to the CR934 (Fig. 3c-
295 e). The exudates of oxalic, malic, and citric acids were significantly higher at the Zehavit in comparison to CR934
296 (Fig. 3f). The results indicate increased biomass, lower pH, higher trichome density, and higher exudate levels in
297 the 'Zehavit' variety.

298

299

300

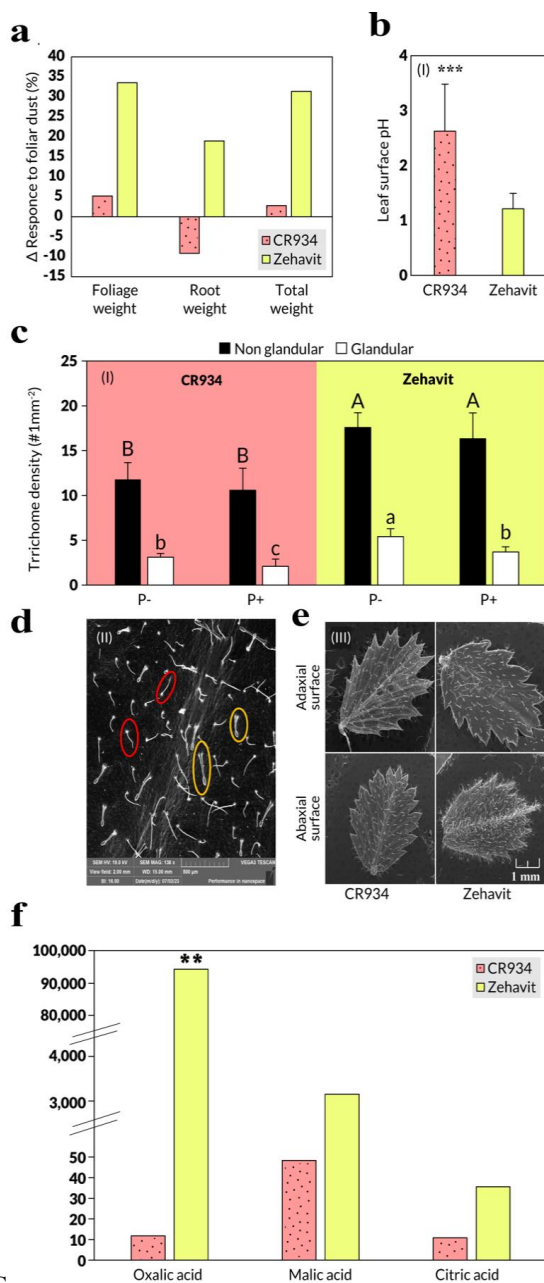


Fig. 3 Comparison of two chickpea varieties - CR934 (dotted, pink) and Zehavit (yellow) and their leaf properties under dust foliar fertilization. (a) Biomass and P uptake response to foliar dust P. Each column indicates the difference Δ (%) between the foliar dusted plants and the control untreated plants ($n=6$). (b) (I) Leaf surface pH. Each value indicates an average of five measurements on a plant throughout the growth season in control treatment ($n=90$), and two measurements in foliar dust treatment ($n=10$). One asterisk indicates significant differences between treatments using a T-test, and a one-way ANOVA ($P \leq 0.05$). Three asterisks indicate significant differences between treatments using a T-test, and a one-way ANOVA ($P \leq 0.001$). (c) Leaf non-Glandular (black column) and glandular (white column) trichome density in CR934 and Zehavit control plants (-P and +P). Different letters indicate significant differences between varieties and treatments using Tukey-HSD test ($P \leq 0.05$) ($n=12$). Capital letters refer to non-glandular trichomes and small letters refer to glandular trichomes. (d). SEM scans of non-glandular (red circles) and glandular (yellow circles) trichomes of typical Zehavit leaf. (e). SEM scans of leaves of CR934 (left) and Zehavit (right) varieties. The Zehavit clearly shows higher density of trichomes in the abaxial surface, rendering it as more fit to extract nutrients from dust particles. (f). Exudates of organic acids. Each column indicates the average of leaf washing from four plants, in P- control treatment ($n=4$). Two asterisks indicate significant differences between treatments using a T-test, and a one-way ANOVA ($P \leq 0.01$). Values are concentrations compared with an internal standard.

301 C

302

303 **Nd isotopic analysis of the dusts, control plants and the treated plants**

304 We utilized the ratio of $^{143}\text{Nd}/^{144}\text{Nd}$ in the ϵNd notation to trace the source of Nd in our experiments and quantify
 305 the flux of dust-borne Nd to plants as an indirect measure of dust nutrient transfer (Fig. 4). The mineral dust

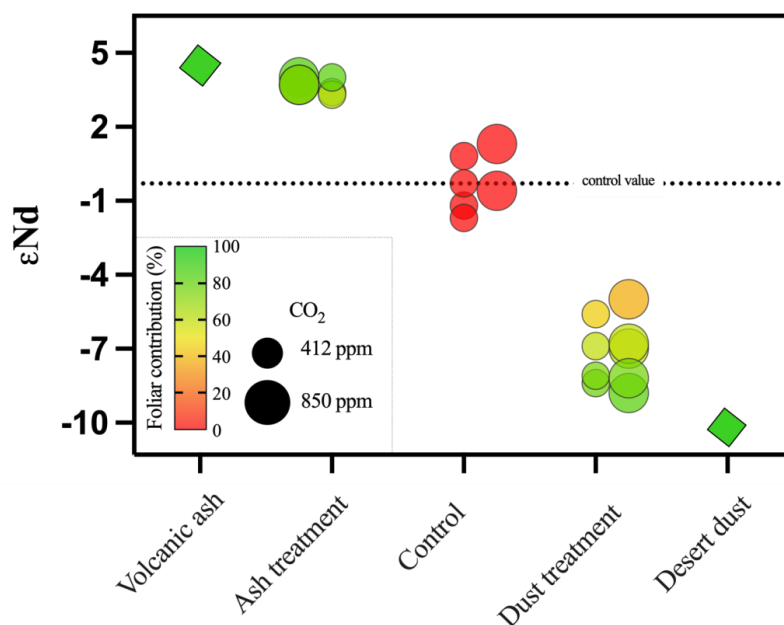


306 analogues presented ϵNd values of 5 and -11 for the volcanic ash and the desert dust, respectively. Plant material
307 ϵNd values of the control plants, that reflect the inheritance value (i.e., arising from the seed Nd isotope
308 composition) was -0.3, desert dust treated plants were characterized with values of -8.8 to -5, and the volcanic ash
309 treated plants were characterized with values of 3.4 to 4. Both treated plant groups are significantly different than
310 the inheritance value of -0.3 characterizing the control group.

311



312



313

314 **Fig. 4** Quantification of dust mineral-nutrient flux from the foliage. Radiogenic isotopic ratios of $^{143}\text{Nd}/^{144}\text{Nd}$ in the different
315 sample groups (x-axis) expressed in ϵNd values. Diamonds represent the two applied mineral fractions of volcanic ash and
316 desert dust; circles represent plants treated with the desert and volcanic dusts and the control groups. Large circles represent
317 plants growing in the 850 ppm eCO_2 and small circles represent the 412 ppm aCO_2 . The color scale reflects the % contribution
318 of Nd originating from the dusts via the foliage, which was calculated using a two-component mixing model. The control
319 plants' Nd signature reflects the inheritance value from the seed, where a value of $\epsilon\text{Nd}=-0.3$ is set as the control, $\epsilon\text{Nd}=-10.3$
320 as the desert dust value, and $\epsilon\text{Nd}=4.6$ as the volcanic ash value. A foliar contribution of more than 60% is evident in the plants
321 applied with desert dust and more than 70% in the plants applied with volcanic ash. Standard errors on the isotopic values are
322 all smaller than the depicted data points.

323

324 Discussion

325

326 Foliar mineral-nutrients uptake

327 In our experiments, we simulated desert dust and volcanic ash deposition by manually applying them on chickpea
328 plants (*Cicer arietinum* cv 'Zehavit'). The dust was applied separately either on the surface of the pot near the
329 roots, or on its foliage (Fig. 1), while control plants were not treated with dust. After several weeks, a significant
330 impact of the foliar treatment was already noticeable where shoot biomass and total P content in the foliage-treated
331 plants had increased, following dusts treatment, compared with the control group. In contrast, the root-treated
332 plants did not show any increases in the biomass or P content, suggesting that over short timescales (i.e., several



333 weeks), foliar uptake is the only nutrient uptake pathway from freshly deposited dust (Fig. 1c, e). These results
334 were then replicated when a similar experiment was conducted with plants grown on sandy soil, in bigger pots
335 (Fig. S1), emphasizing that our observations are not limited to the specific artificial experimental conditions in
336 perlite (which may bias root behavior), but also apply for real soil conditions (Fig. S1).

337 **Plant strategies for foliar mineral-nutrient uptake**

338 Most of the P in the dusts is incorporated in the mineral lattice of minerals such as apatite (Dam et al., 2021),
339 which is largely insoluble under the natural rhizosphere pH range (Hinsinger, 2001)(Hinsinger, 2001). Hence, P
340 in volcanic or desert dust has low bioavailability for root uptake as was also shown in Lokshin et al. (2024a) with
341 fire ash. On the leaf surface however, chemical, morphological, and microbial modifications may promote nutrient
342 solubility and bioavailability and thus enable uptake through the leaf surface (Gross et al., 2021; Muhammad et
343 al., 2019)(Gross et al., 2021; Muhammad et al., 2019). Examining two chickpea varieties with contrasting
344 responses to dust application: wild variety CR934, and common domesticated variety Zehavit, we found a few
345 properties that facilitate foliar P acquisition from dust (Fig. 3). These include structural, morphological, and
346 chemical modifications that are comparable to those reported in the rhizosphere (Hinsinger, 2001)(Hinsinger,
347 2001). The foliar-uptake-efficient variety Zehavit has significantly more acidic leaf surface (pH ~ 1, Fig. 3b), and
348 thus promotes both dissolution and mobility of P from the pH sensitive mineral apatite (Gross et al., 2015)(Gross
349 et al., 2015), as well as other mineral-nutrients in the dust (Bradl, 2004; Gross et al., 2021; Muhammad et al.,
350 2019)(Bradl, 2004; Gross et al., 2021; Muhammad et al., 2019). Additionally, a unique set of metabolites secreted
351 from the leaf surface further facilitated the foliar uptake pathway in Zehavit. These include increased
352 concentrations of oxalate and malate, which are known to release insoluble P in soils through anion exchange
353 reactions (Lambers et al., 2019; Tiwari et al., 2022)(Lambers et al., 2019; Tiwari et al., 2022), and increased levels
354 of sugars such as glucose and sucrose that may promote the activity of nutrient solubilizing microbes on the
355 phyllosphere (Shakir et al., 2021)(Shakir et al., 2021) (Fig. 3f, fig. S2). We further found that Zehavit showed
356 higher leaf trichome density on both leaf axial and adaxial sides (Fig. 3 c,d,e). These trichomes facilitate the
357 release of metabolites and promote adhesion of dust captured on leaf surfaces (fig. S3) (Gross et al., 2021)(Gross
358 et al., 2021). We postulate that other plant species share comparable leaf traits that enhance dust capture and
359 solubility such as wheat and various tree species that showed strong responses to foliar dust fertilization (Gross et
360 al., 2021; Starr et al., 2023)(Gross et al., 2021; Starr et al., 2023). Overall, our results suggest that the combination
361 of leaf surface acidification, secretion of organic acids and additional exudations combined with an increased
362 trichome density enhances foliar dust capture and nutrient uptake in chickpeas. Results of previous study with
363 application of inert silicon powder on chickpea leaf surface indicate that the shading effect resulting leaf surface
364 coverage with dust has low effect on plant growth and photosynthesis (Gross et al. (2021). Yet, the dust shading
365 effect was more pronounced in several tree species (Starr *et al.*, 2023), suggesting the contrasting impact of
366 coverage of the foliage should be considered.

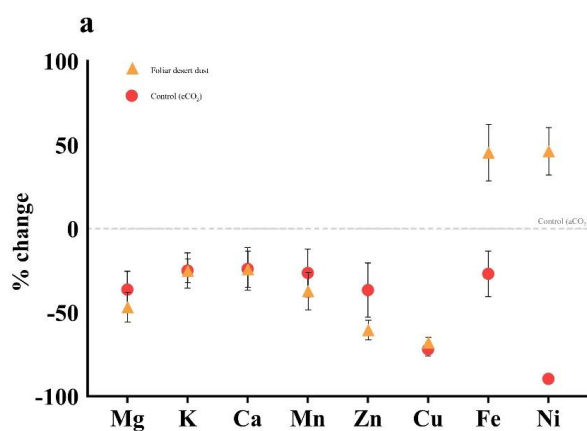
367 **Dust impact on plant nutrient status under eCO₂**

368 Numerous studies reported that eCO₂ conditions reduce the concentrations of several nutrients in plant tissues
369 such as Fe, Zn, Cu, Mn, Ni and others (Loladze, 2002; Fernando et al., 2014; Myers *et al.*, 2014; Gojon *et al.*,
370 2023). The reduction in shoot nutrient concentrations was also observed in our experiments (fig. 5). In accordance



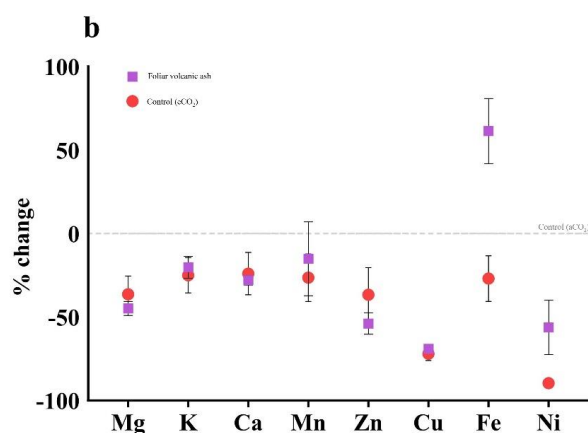
371 with previous knowledge (Loladze, 2002)(Loladze, 2002), plants that were grown under eCO₂ in our experiment
372 showed a significant reduction of 10-50% in the concentrations of nutrients such as Mg, K, Ca, Mn, Zn and Fe,
373 with even more significant reductions in Cu and Ni (72% and 90%, respectively), (Fig. 5). Although we did not
374 observe statistically significant differences in biomass between control plants grown under aCO₂ and eCO₂
375 conditions (P = 0.4), the reduction in essential macro- and micronutrient concentrations may be partly explained
376 by the effect of nutrient dilution. Another potential reason for the nutrient decline under eCO₂ could be related to
377 reduced efficiency in mineral nutrient absorption through the root system (Gojon et al., 2023). Click or tap here
378 to enter text. Click or tap here to enter text.. We found that foliar application of both volcanic and desert
379 dust on plants that were grown under eCO₂ replenished their Fe and Ni concentrations (both essential
380 micronutrients for plant growth and in the human diet) compared with the control group (fig. 5a,b). Desert dust
381 treated plants showed increases of Fe and Ni concentrations of 44% and 46%, respectively (Fig. 5a). Volcanic ash
382 treated plants showed Fe elevated concentrations of 66% (Fig. 5b). The Ni concentrations had more moderate
383 increases from volcanic ash, with 40% higher than in the aCO₂. These increases returned Fe and Ni back to
384 standard, nontoxic levels (Shahzad et al. 2018). These results emphasize that the role foliar uptake of atmospheric
385 nutrients on the mineral nutrition level of plants will be greater under eCO₂ and offset the projected nutrient
386 reduction driven by the dilution effect and the downregulation of the root's nutrient uptake pathway (Zhu et al.,
387 2018)(Zhu et al., 2018).

388
389





397



406 **Fig. 5** Comparison of the % change in plant nutrient concentration under eCO₂ compared with aCO₂ control plants. The
407 comparison was conducted as follows: the average value of each nutrient in plants grown under aCO₂ was calculated, and then
408 each nutrient in individual chickpea plants grown under eCO₂ levels was expressed as a ratio relative to the average under
409 aCO₂ conditions ($\text{eCO}_2 \text{ plant (each individual plant)} / \text{aCO}_2 \text{ plant (average of all the control plants)}$). Changes in nutrient concentrations of
410 the control eCO₂ plants (red circles) show that eCO₂ conditions deteriorate plant nutritional status significantly. (a) The effect
411 of foliar treatment of desert dust (orange triangles). (b) The effect of foliar treatment of volcanic ash (purple squares). Error
412 bars denote SD.

413

414 **Quantifying the contribution of foliar nutrient uptake from dust**

415 Traditionally, radiogenic Nd isotopes serve as excellent tracers for sources of magmatic rocks (Stein and
416 Goldstein, 1996)(Stein and Goldstein, 1996), sediment archives (Chadwick et al., 1999; Palchan et al.,
417 2018)(Chadwick et al., 1999; Palchan et al., 2018), and water bodies (Farmer et al., 2019)(Farmer et al., 2019).
418 Since Nd is found in high concentration in nutrient bearing minerals (Aciego et al., 2017; Arvin et al., 2017;
419 Chadwick et al., 1999)(Aciego et al., 2017; Arvin et al., 2017; Chadwick et al., 1999), Nd isotopes were recently
420 used to trace P sources in plant tissues, where it was shown that the contribution of dust outpaces the weathering
421 of the local bedrock over geological time scales (Aciego et al., 2017; Arvin et al., 2017)(Aciego et al., 2017; Arvin
422 et al., 2017). While the use of Nd isotopes to other elements such as P provides new knowledge on their sources,
423 it should be done cautiously because different elements have differing speciation, uptake mechanisms, and
424 transport kinetics in plant tissue. Here, we utilized the ratio of ¹⁴³Nd/¹⁴⁴Nd in the εNd notation to trace the source
425 of Nd in our experiments and quantify its flux to plant tissue from dust. From this measurement we can
426 approximate the flux of P, Fe and Ni via foliar pathway (Fig. 4). We used a two-component mixing model, where
427 the average εNd value of the control plants, -0.3, which arise from the Nd “inheritance” (i.e., the Nd composition
428 of the seed) is regarded as one end member, and dust εNd values are regarded as the second end member, with
429 values of -11 (desert dust) and 5 (volcanic ash). We found that desert dust treated plants were characterized with
430 εNd values of -8.8 to -5, significantly different than the inheritance value of the control group. Similarly, the



431 volcanic ash treated plants were characterized with ϵNd values of 3.4 to 4, significantly different than the
432 inheritance value of -0.3. Thus, it is evident that the ϵNd of the foliage-treated plants comprise a mixture of the
433 inheritance and the type of dust applied. Based on the mixing model, the chickpea plant acquired over 60% of its
434 Nd from desert dust deposited on the foliage. Volcanic ash deposited on the foliage contributed over 70% of its
435 Nd (Fig. 4). However, Nd isotopes do not show the increased supplement of Fe and Ni in plants that were grown
436 under $e\text{CO}_2$. Thus, more data on the relation between Nd and other nutrients uptake will advance its use in future
437 studies to quantify the immediate contribution of freshly deposited dust on plants nutrition in field and lab
438 experimental settings.

439
440 In conclusion, we showed here that dust nutrient uptake via the foliar pathway in chickpea plants plays a major
441 role in their nutrition. Plant foliage captures and dissolves freshly deposited dust particles, making atmospheric
442 mineral nutrients more accessible through the foliage on a short time scale than via the roots. Most of the P in the
443 dust is incorporated in the mineral lattice of minerals such as apatite (Dam et al., 2021)(Dam et al., 2021), which
444 is largely insoluble under the natural rhizosphere pH range (Hinsinger, 2001)(Hinsinger, 2001). Hence, P in dust
445 has low bioavailability for root uptake. On the leaf surface however, chemical, morphological, and microbial
446 modifications may promote nutrient solubility and bioavailability and facilitate uptake through the leaf surface
447 (Gross et al., 2021; Muhammad et al., 2019)(Gross et al., 2021; Muhammad et al., 2019). Thus, our findings
448 highlight that dust serves as an alternative source of nutrients to plants from the foliage on short timescales of a
449 few weeks. Furthermore, that foliar dust acquisition compensates for the reduction in nutrients such as Fe and Ni,
450 induced by $e\text{CO}_2$ conditions (Gojon et al., 2023)(Gojon et al., 2023). The broader aspect of our findings
451 emphasizes the central role of dust in plant nutrition through the foliar pathway and to global biogeochemical
452 cycles. Our findings imply that the foliar nutrient uptake pathway from natural dust will play a central role in
453 $e\text{CO}_2$ earth, and that this pathway may be a target for novel fertilization techniques to compensate for the expected
454 decline in the crops' nutritional value.

455

456

457

458 **Acknowledgments**

459

460 We thank Dr. Yigal Erel and Ofir Tirosh from the Hebrew University of Jerusalem for their support in ICP-MS
461 analyses, and Dr. Yael Kiro from Weismann Institute for conducting isotopic chromatography in her lab, and
462 Dr. Stephen Fox for his support in MC-ICP-MS analyses.

463 **Author Contributions:**

464 Conceptualization: DP, AG, RE

465 Dust sampling: AL, DA, AG

466 Methodology: DP, AG, RE

467 Investigation: AL, EG, SF



468 Visualization: DP, AL, EG

469 Funding acquisition: AG, RE, AL

470 Project administration: DP, AG

471 Supervision: DP, AG, RE

472 Writing – original draft: DP, AG, AL, RE

473 **Competing Interest Statement:** The authors declare no competing interests.

474 **Classification:** Physical Sciences - Earth, Atmospheric, and Planetary Sciences; Biological Sciences - Plant
475 Biology.

476

477

478 **References**

479 Aciego, S. M., Riebe, C. S., Hart, S. C., Blakowski, M. A., Carey, C. J., Aarons, S. M., Dove, N. C.,
480 Botthoff, J. K., Sims, K. W. W., and Aronson, E. L.: Dust outpaces bedrock in nutrient supply to
481 montane forest ecosystems, *Nat Commun*, 8, 14800, <https://doi.org/10.1038/ncomms14800>,
482 2017.

483 Arvin, L. J., Riebe, C. S., Aciego, S. M., and Blakowski, M. A.: Global patterns of dust and
484 bedrock nutrient supply to montane ecosystems, *Sci Adv*, 3, eaa01588,
485 <https://doi.org/10.1126/sciadv.aao1588>, 2017.

486 Bauters, M., Drake, T. W., Wagner, S., Baumgartner, S., Makelele, I. A., Bodé, S., Verheyen, K.,
487 Verbeeck, H., Ewango, C., Cizungu, L., Van Oost, K., and Boeckx, P.: Fire-derived phosphorus
488 fertilization of African tropical forests, *Nat Commun*, 12, <https://doi.org/10.1038/S41467-021-25428-3>, 2021.

490 Bradl, H. B.: Adsorption of heavy metal ions on soils and soils constituents, *J Colloid Interface*
491 *Sci*, 277, 1–18, <https://doi.org/10.1016/J.JCIS.2004.04.005>, 2004.

492 Chadwick, O. A., Derry, L. A., Vitousek, P. M., Huebert, B. J., and Hedin, L. O.: Changing sources
493 of nutrients during four million years of ecosystem development, *Nature*, 397, 491–497,
494 <https://doi.org/10.1038/17276>, 1999.

495 Ciriminna, R., Scurria, A., Tizza, G., and Pagliaro, M.: Volcanic ash as multi-nutrient mineral
496 fertilizer: Science and early applications, *JSFA Reports*, 2, 528–534,
497 <https://doi.org/10.1002/JSF2.87>, 2022.

498 Clarkson, D. T. and Hanson, J. B.: THE MINERAL NUTRITION OF HIGHER PLANTS, *Ann. Rev.*
499 *Plant Physiol*, 31, 239–98, 1980.

500 Dam, T. T. N., Angert, A., Krom, M. D., Bigio, L., Hu, Y., Beyer, K. A., Mayol-Bracero, O. L.,
501 Santos-Figueroa, G., Pio, C., and Zhu, M.: X-ray Spectroscopic Quantification of Phosphorus
502 Transformation in Saharan Dust during Trans-Atlantic Dust Transport, *Cite This: Environ. Sci.*
503 *Technol*, 55, 12694–12703, <https://doi.org/10.1021/acs.est.1c01573>, 2021.



- 504 Eger, A., Almond, P. C., and Condron, L. M.: Phosphorus fertilization by active dust deposition
505 in a super-humid, temperate environment—Soil phosphorus fractionation and accession
506 processes, *Global Biogeochem Cycles*, 27, 108–118, <https://doi.org/10.1002/GBC.20019>,
507 2013.
- 508 Farmer, J. R., Hönlisch, B., Haynes, L. L., Kroon, D., Jung, S., Ford, H. L., Raymo, M. E., Jaume-
509 Seguí, M., Bell, D. B., Goldstein, S. L., Pena, L. D., Yehudai, M., and Kim, J.: Deep Atlantic Ocean
510 carbon storage and the rise of 100,000-year glacial cycles, *Nature Geoscience* 2019 12:5, 12,
511 355–360, <https://doi.org/10.1038/s41561-019-0334-6>, 2019.
- 512 Gojon, A., Cassan, O., Bach, L., Lejay, L., and Martin, A.: The decline of plant mineral nutrition
513 under rising CO₂: physiological and molecular aspects of a bad deal, *Trends Plant Sci*, 28, 185–
514 198, <https://doi.org/10.1016/J.TPLANTS.2022.09.002>, 2023.
- 515 Goll, D. S., Bauters, M., Zhang, H., Ciais, P., Balkanski, Y., Wang, R., and Verbeeck, H.:
516 Atmospheric phosphorus deposition amplifies carbon sinks in simulations of a tropical forest in
517 Central Africa, *New Phytologist*, 237, 2054–2068, <https://doi.org/10.1111/NPH.18535>, 2023.
- 518 Gross, A., Goren, T., Pio, C., Cardoso, J., Tirosh, O., Todd, M. C., Rosenfeld, D., Weiner, T.,
519 Custodio, D., and Angert, A.: Variability in Sources and Concentrations of Saharan Dust
520 Phosphorus over the Atlantic Ocean, *Environ Sci Technol Lett*, 2, 31–37,
521 <https://doi.org/10.1021/ez500399z>, 2015.
- 522 Gross, A., Palchan, D., Krom, M. D., and Angert, A.: Elemental and isotopic composition of
523 surface soils from key Saharan dust sources, *Chem Geol*, 442, 54–61,
524 <https://doi.org/10.1016/j.chemgeo.2016.09.001>, 2016a.
- 525 Gross, A., Turner, B. L., Goren, T., Berry, A., and Angert, A.: Tracing the Sources of Atmospheric
526 Phosphorus Deposition to a Tropical Rain Forest in Panama Using Stable Oxygen Isotopes,
527 *Environ Sci Technol*, 50, 1147–1156, <https://doi.org/10.1021/ACS.EST.5B04936>, 2016b.
- 528 Gross, A., Tiwari, S., Shtein, I., and Erel, R.: Direct foliar uptake of phosphorus from desert dust,
529 *New Phytologist*, 230, 2213–2225, <https://doi.org/10.1111/nph.17344>, 2021a.
- 530 Gross, A., Tiwari, S., Shtein, I., and Erel, R.: Direct foliar uptake of phosphorus from desert dust,
531 *New Phytologist*, 230, 2213–2225, <https://doi.org/10.1111/NPH.17344>, 2021b.
- 532 Guieu, C., Dulac, F., Desboeufs, K., Wagener, T., Pulido-Villena, E., Grisoni, J. M., Louis, F.,
533 Ridame, C., Blain, S., Brunet, C., Bon Nguyen, E., Tran, S., Labiadh, M., and Dominici, J. M.:
534 Large clean mesocosms and simulated dust deposition: A new methodology to investigate
535 responses of marine oligotrophic ecosystems to atmospheric inputs, *Biogeosciences*, 7, 2765–
536 2784, <https://doi.org/10.5194/BG-7-2765-2010>, 2010.
- 537 Hinsinger, P.: Bioavailability of soil inorganic P in the rhizosphere as affected by root-induced
538 chemical changes: A review, *Plant Soil*, 237, 173–195,
539 <https://doi.org/10.1023/A:1013351617532/METRICS>, 2001.
- 540 Jweda, J., Bolge, L., Class, C., and Goldstein, S. L.: High Precision Sr-Nd-Hf-Pb Isotopic
541 Compositions of USGS Reference Material BCR-2, *Geostand Geoanal Res*, 40, 101–115,
542 <https://doi.org/10.1111/j.1751-908X.2015.00342.x>, 2016.
- 543 Kok, J. F., Adebijoyi, A. A., Albani, S., Balkanski, Y., Checa-Garcia, R., Chin, M., Colarco, P. R.,
544 Hamilton, D. S., Huang, Y., Ito, A., Klose, M., Li, L., Mahowald, N. M., Miller, R. L., Obiso, V.,
545 Pérez García-Pando, C., Rocha-Lima, A., and Wan, J. S.: Contribution of the world’s main dust



- 546 source regions to the global cycle of desert dust, *Atmos Chem Phys*, 21, 8169–8193,
547 <https://doi.org/10.5194/ACP-21-8169-2021>, 2021.
- 548 Lal, R.: Soil degradation as a reason for inadequate human nutrition, *Food Secur*, 1, 45–57,
549 <https://doi.org/10.1007/S12571-009-0009-Z>, 2009.
- 550 Lambers, H., Albornoz, F. E., Arruda, A. J., Barker, T., Finnegan, P. M., Gille, C., Gooding, H.,
551 Png, K., Ranathunge, K., and Zhong, H.: Nutrient-acquisition strategies, in: *A Jewel in the crown*
552 *of a global biodiversity hotspot*, edited by: Lambers, H., Kwongan Foundation and the Western
553 Australian Naturalists' Club Inc., Perth, 2019.
- 554 Van Langenhove, L., Verryckt, L. T., Bréchet, L., Courtois, E. A., Stahl, C., Hofhansl, F., Bauters,
555 M., Sardans, J., Boeckx, P., Fransen, E., Peñuelas, J., and Janssens, I. A.: Atmospheric
556 deposition of elements and its relevance for nutrient budgets of tropical forests, 149, 175–193,
557 <https://doi.org/10.1007/s10533-020-00673-8>, 2020.
- 558 Langmann, B.: Volcanic Ash versus Mineral Dust: Atmospheric Processing and Environmental
559 and Climate Impacts, *ISRN Atmospheric Sciences*, 2013, 1–17,
560 <https://doi.org/10.1155/2013/245076>, 2013a.
- 561 Langmann, B.: Volcanic Ash versus Mineral Dust: Atmospheric Processing and Environmental
562 and Climate Impacts, *ISRN Atmospheric Sciences*, 2013, 1–17,
563 <https://doi.org/10.1155/2013/245076>, 2013b.
- 564 Lokshin, A., Palchan, D., and Gross, A.: Direct foliar phosphorus uptake from wildfire ash,
565 *Biogeosciences*, 21, 2355–2365, <https://doi.org/10.5194/BG-21-2355-2024>, 2024a.
- 566 Lokshin, A., Gross, A., Dor, Y. Ben, and Palchan, D.: Rare earth elements as a tool to study the
567 foliar nutrient uptake phenomenon under ambient and elevated atmospheric CO₂
568 concentration, *Science of The Total Environment*, 948, 174695,
569 <https://doi.org/10.1016/J.SCITOTENV.2024.174695>, 2024b.
- 570 Loladze, I.: Rising atmospheric CO₂ and human nutrition: toward globally imbalanced plant
571 stoichiometry?, *Trends Ecol Evol*, 17, 457–461, [https://doi.org/10.1016/S0169-5347\(02\)02587-](https://doi.org/10.1016/S0169-5347(02)02587-9)
572 9, 2002.
- 573 Loladze, I.: Hidden shift of the ionome of plants exposed to elevated CO₂ depletes minerals at
574 the base of human nutrition, *Elife*, 2014, <https://doi.org/10.7554/ELIFE.02245>, 2014.
- 575 Longo, A. F., Ingall, E. D., Diaz, J. M., Oakes, M., King, L. E., Nenes, A., Mihalopoulos, N., Violaki,
576 K., Avila, A., and Benitez-Nelson, C. R.: P-NEXFS analysis of aerosol phosphorus delivered to
577 the Mediterranean Sea, *Geophys Res Lett*, 41, 4043–4049, 2014.
- 578 Lowe, N. M.: The global challenge of hidden hunger: perspectives from the field, *Proceedings of*
579 *the Nutrition Society*, 80, 283–289, <https://doi.org/10.1017/S0029665121000902>, 2021.
- 580 Marschner, H., Kirkby, E. A., and Engels, C.: Importance of Cycling and Recycling of Mineral
581 Nutrients within Plants for Growth and Development, *Botanica Acta*, 110, 265–273,
582 <https://doi.org/10.1111/J.1438-8677.1997.TB00639.X>, 1997.
- 583 Muhammad, S., Wuyts, K., and Samson, R.: Atmospheric net particle accumulation on 96 plant
584 species with contrasting morphological and anatomical leaf characteristics in a common
585 garden experiment, *Atmos Environ*, 202, 328–344,
586 <https://doi.org/10.1016/J.ATMOENV.2019.01.015>, 2019.



- 587 Myers, S. S., Zanobetti, A., Kloog, I., Huybers, P., Leakey, A. D. B., Bloom, A. J., Carlisle, E.,
588 Dietterich, L. H., Fitzgerald, G., Hasegawa, T., Holbrook, N. M., Nelson, R. L., Ottman, M. J.,
589 Raboy, V., Sakai, H., Sartor, K. A., Schwartz, J., Seneweera, S., Tausz, M., and Usui, Y.:
590 Increasing CO₂ threatens human nutrition, *Nature* 2014 510:7503, 510, 139–142,
591 <https://doi.org/10.1038/nature13179>, 2014.
- 592 Nakamaru, Y., Nanzyo, M., and Yamasaki, S. I.: Utilization of apatite in fresh volcanic ash by
593 pigeonpea and chickpea, *Soil Sci Plant Nutr*, 46, 591–600,
594 <https://doi.org/10.1080/00380768.2000.10409124>, 2000.
- 595 Okin, G. S., Mahowald, N., Chadwick, O. A., and Artaxo, P.: Impact of desert dust on the
596 biogeochemistry of phosphorus in terrestrial ecosystems, *Global Biogeochem Cycles*, 18,
597 <https://doi.org/10.1029/2003GB002145>, 2004.
- 598 Van Oss, R., Abbo, S., Eshed, R., Sherman, A., Coyne, C. J., Vandemark, G. J., Zhang, H. Bin, and
599 Peleg, Z.: Genetic relationship in cicer Sp. expose evidence for geneflow between the cultigen
600 and its wild progenitor, *PLoS One*, 10, <https://doi.org/10.1371/journal.pone.0139789>, 2015.
- 601 Palchan, D., Stein, M., Almogi-Labin, A., Erel, Y., and Goldstein, S. L.: Dust transport and
602 synoptic conditions over the Sahara–Arabia deserts during the MIS6/5 and 2/1 transitions from
603 grain-size, chemical and isotopic properties of Red Sea cores, *Earth Planet Sci Lett*, 382, 125–
604 139, <https://doi.org/10.1016/j.epsl.2013.09.013>, 2013.
- 605 Palchan, D., Erel, Y., and Stein, M.: Geochemical characterization of contemporary fine detritus
606 in the Dead Sea watershed, *Chem Geol*, 494, 30–42,
607 <https://doi.org/10.1016/J.CHEMGEO.2018.07.013>, 2018.
- 608 Shakir, S., Zaidi, S. S. e. A., de Vries, F. T., and Mansoor, S.: Plant Genetic Networks Shaping
609 Phyllosphere Microbial Community, <https://doi.org/10.1016/j.tig.2020.09.010>, 1 April 2021.
- 610 Starr, M., Klein, T., and Gross, A.: Direct foliar acquisition of desert dust phosphorus fertilizes
611 forest trees despite reducing photosynthesis, *Tree Physiol*, 43, 794–804,
612 <https://doi.org/10.1093/TREEPHYS/TPAD012>, 2023.
- 613 St.Clair, S. B. and Lynch, J. P.: The opening of Pandora’s Box: climate change impacts on soil
614 fertility and crop nutrition in developing countries, 335, 101–115, <https://doi.org/10.1007/s>,
615 2010.
- 616 Stein, M. and Goldstein, S. L.: From plume head to continental lithosphere in the Arabian-
617 Nubian shield, *Nature*, 382, 773–778, 1996.
- 618 Stockdale, A., Krom, M. D., Mortimer, R. J. G., Benning, L. G., Carslaw, K. S., Herbert, R. J., Shi,
619 Z., Myriokefalitakis, S., Kanakidou, M., and Nenes, A.: Understanding the nature of atmospheric
620 acid processing of mineral dusts in supplying bioavailable phosphorus to the oceans,
621 *Proceedings of the National Academy of Sciences*, 113, 14639–14644, 2016.
- 622 Tanaka, T., Togashi, S., Kamioka, H., Amakawa, H., Kagami, H., Hamamoto, T., Yuhara, M.,
623 Orihashi, Y., Yoneda, S., Shimizu, H., Kunimaru, T., Takahashi, K., Yanagi, T., Nakano, T.,
624 Fujimaki, H., Shinjo, R., Asahara, Y., Tanimizu, M., and Dragusanu, C.: JNdi-1: a neodymium
625 isotopic reference in consistency with LaJolla neodymium, *Chem Geol*, 168, 279–281,
626 [https://doi.org/10.1016/S0009-2541\(00\)00198-4](https://doi.org/10.1016/S0009-2541(00)00198-4), 2000.
- 627 Tiwari, S., Erel, R., and Gross, A.: Chemical processes in receiving soils accelerate
628 solubilisation of phosphorus from desert dust and fire ash, *Eur J Soil Sci*, 73,
629 <https://doi.org/10.1111/EJSS.13270>, 2022.



630 Wasserburg, G. J., Jacobsen, S. B., DePaolo, D. J., McCulloch, M. T., and Wen, T.: Precise
631 determination of Sm/Nd ratios, Sm and Nd isotopic abundances in standard solutions,
632 *Geochim Cosmochim Acta*, 45, 2311–2323, [https://doi.org/10.1016/0016-7037\(81\)90085-5](https://doi.org/10.1016/0016-7037(81)90085-5),
633 1981.

634 Zhu, C., Kobayashi, K., Loladze, I., Zhu, J., Jiang, Q., Xu, X., Liu, G., Seneweera, S., Ebi, K. L.,
635 Drewnowski, A., Fukagawa, N. K., and Ziska, L. H.: Carbon dioxide (CO₂) levels this century will
636 alter the protein, micronutrients, and vitamin content of rice grains with potential health
637 consequences for the poorest rice-dependent countries, *Sci Adv*, 4,
638 <https://doi.org/10.1126/SCIADV.AAQ1012>, 2018.

639

640

641

642

643

644

645

646

647

648

649

650

651

652

653 **Availability Statement**

654

655 **All relevant data are included within the manuscript. No additional data, code, or**
656 **software were used or are available beyond what is presented in the paper.**

657

658

659 **Anton Lokshin and the co-authors**



Loell